Proc. of the SPIE Defense and Security Conference, Unmanned Ground Vehicle Technology VII, Orlando, FL, March 28th to April 1st, 2005.

Terrain Trafficability Characterization with a Mobile Robot

Lauro Ojeda
Dept. of Mechanical Engineering
The University of Michigan
Ann Arbor, MI 48109, USA
lojeda@umich.edu
[1] (734) 647-1803

Johann Borenstein
Dept. of Mechanical Engineering
The University of Michigan
Ann Arbor, MI 48109, USA
johannb@umich.edu
[1] (734) 763-1560

Gary Witus
Turing Associates, Inc.
1392 Honey Run Drive
Ann Arbor, MI 48103, USA
witusg@umich.edu
[1] (734) 665-4818

ABSTRACT

Most research on off-road mobile robot sensing focuses on obstacle negotiation, path planning, and position estimation. These issues have conventionally been the foremost factors limiting the performance and speeds of mobile robots. Very little attention has been paid to date to the issue of terrain trafficability, that is, the terrain's ability to support vehicular traffic. Yet, trafficability is of great importance if mobile robots are to reach speeds that human-driven vehicles can reach on rugged terrain. For example, it is obvious that the maximal allowable speed for a turn is lower when driving over sand or wet grass than when driving on packed dirt or asphalt.

This paper presents our work on automated real-time characterization of terrain with regard to trafficability for small mobile robots. The two proposed methods can be implemented on skid-steer mobile robots and possibly also on tracked mobile robots. The paper also presents experimental results for each of the two implemented methods.

Keywords: Mobile, robot, off-road, terrain, characterization, trafficability.

1. INTRODUCTION

Terrain characterization has been the subject of several studies. Perhaps the best known and widely cited work is that of Bekker [1956; 1960; 1969] and Wong [1967]. From the point of view of terramechanics, soil can be characterized by determining the terrain parameters. Many approaches to terrain characterization require offline analysis and/or dedicated equipment [Nohse, et al., 1991; Shmulevich, et al., 1996]. Terrain characterization without dedicated equipment was proposed by [Matijevic. et al., 1997] for the Sojourner rover and its 1997 Mars mission. Based on this method, Sojourner used one of its wheels to characterize terrain.

A real-time approach based on the measurement of wheel sinkage in soft soil using a video camera was proposed by [Iagnemma, et.al., 2004]. Other researchers approached the terrain classification problem based on the terrain's visual or topographic appearance. These methods are collectively called vision-based techniques and generally use video cameras or range sensors [Manduchi, et al., 2004; Vandapel, et al., 2004].

In this paper we propose two fully self-contained terrain characterization methods for skid-steer mobile robots. With "self-contained" we mean that our system does not require any special-purpose instruments to be attached to the robot. Rather, the proposed methods monitor typical onboard sensors, such as gyros and motor current sensors. The unique advantage of this approach is that our method can be applied during real-time and during an actual robot mission.

In order to develop the classification method, we instrumented a Pioneer 2-AT (P2AT) with three gyros, accelerometers, and motor current sensors. In extensive tests we collected data on a variety of different terrains, such as gravel, sand, asphalt, grass, and dirt. Sensor data was collected while the robot performed carefully prescribed maneuvers. We then analyzed the data with two different methods, each of which yields a curve that is characteristic for a particular terrain. We describe these methods in Sections 2 and 3. Section 4 provides experimental results.

2. MOTOR CURRENT VS. RATE-BASED (MCR) TERRAIN ANALYSIS

In the science of terramechanics, terrain properties are often expressed by stress-strain relationships. Data for stress-strain analysis is generally obtained through the use of an instrument called "bevameter." Figure 1 shows the main functional component of a bevameter: an annular plate with radial grousers that engage the terrain. Not shown is an electric motor that rotates the plate.

Among other parameters of interest, a bevameter can be used to evaluate the horizontal stress-strain relationship of a given terrain. The shear-stress vs. shear-displacement relationship is obtained based on measurements of torque and angular displacement of the annular plate as a function of the normal stress. For many surfaces it can be described by an exponential function [Janosi and Hanamoto, 1961]:

$$\tau = (c + \sigma \tan\varphi)\left(1 - e^{-\frac{j}{K}}\right) \qquad (1)$$

where

j – Shear displacement

K – Shear deformation modulus

σ – Normal stress

φ – internal friction angle of the soil

c – cohesion of the soil

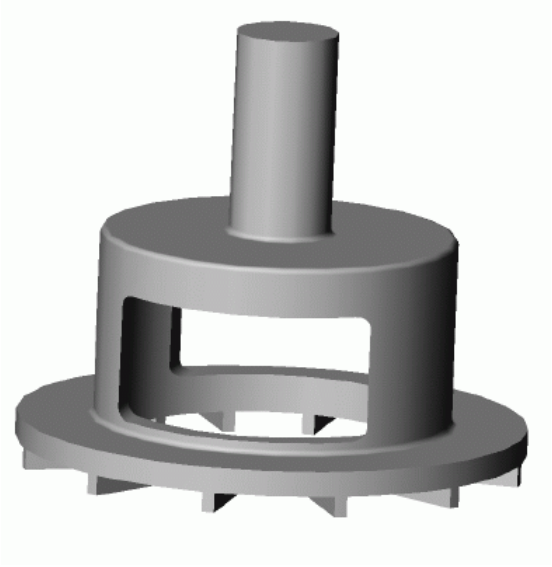

Figure 1: An annular shear plate is used in bevameters to determine shear stress vs. shear displacement. The plate is pressed into the terrain surface and rotated by a motor. Shear stress is measured by monitoring the torque required to rotate the shear plate.

According to the Coulomb-Mohr soil failure criterion, *total* displacement occurs when the shear stress applied to a given terrain exceeds the maximum shear stress that the terrain can bear, τ_{max} (see Figure 2):

$$\tau_{max} = c + \sigma_{max} \tan\varphi \qquad (2)$$

where

σ_{max} – maximal normal component of the stress region at the wheel-terrain interface

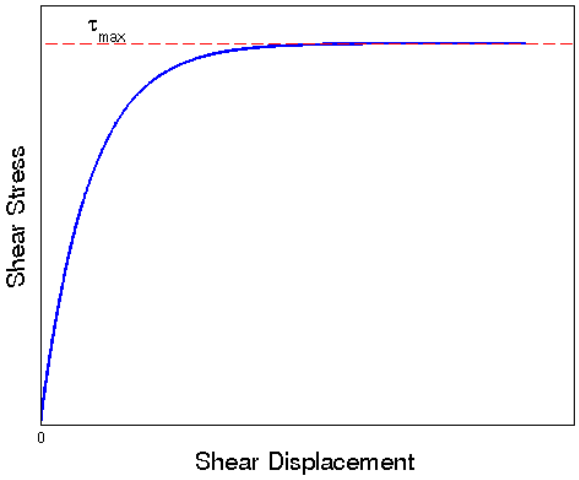

Figure 2: Typical shear-stress vs. shear-displacement curve.

The parameters c and φ cannot be obtained from a single shear-stress vs. shear-displacement curve. Rather, these parameters are estimated using the so-called Mohr circles based on the Coulomb's criterion of soil failure. This criterion is established based on the strain-stress relationship $\tau(j)$ under different normal loads σ (see detailed discussion in [TERZAGHI, 1994]).

As a modification of the conventional method for determining the horizontal strain-stress relationship, we propose a method that uses a skid-steer mobile robot instead of a bevameter. In the work presented here we used a Pioneer 2-AT (P2AT) to determine the horizontal strain-stress relationship. When a skid-steer vehicle turns, the wheels are forced to slip. This motion is similar to that of the annular plate of a bevameter. The torque needed to overcome the friction between the wheels and the ground can be estimated by measuring motor currents, and an onboard gyroscope can be used to determine the angular displacement. The *Motor Currents versus Rate-of-turn* (abbreviated "MCR" in the remainder of this paper) relationship can be used analogously to the shear-stress vs. shear-displacement. One limitation of our method is that since the weight of the robot is constant, the normal load will not change, and we can only generate

one single characteristic MCR curve. Therefore, the Mohr circles can not be constructed. Nonetheless, we believe that one single characteristic MCR curve contains enough information to classify the terrain.

In a proof-of-concept experiment, performed on pavement, we commanded the P2AT to move at a constant linear speed of 200 mm/sec, while the rate of turn was increased every 5 seconds. Figure 3 shows the MCR curve characteristic obtained for this surface. In this plot, the x-axis represents the angular rate of the robot as measured by the gyroscope and the y-axis is the average motor current. Each of the ~15 data points corresponds to an average of 5 seconds of data. Therefore, each individual curve can be created in an experiment that lasts about 75 seconds. The obvious shortcoming of this approach is that the robot has to perform many turns while collecting data. In addition, this kind of experiment needs a relatively large physical space to be performed. The method, as described, is therefore not particularly suitable for terrain characterization in real-time, during an actual robot mission. Two other methods, discussed in detail in Section 3, overcome this limitation and are thus suitable for real-time implementations.

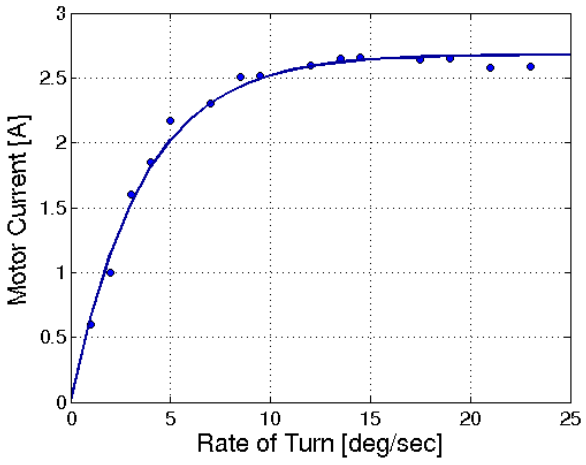

Figure 3: Curve characteristic for pavement. The blue dots are actual data points (each representing the average motor current over 5 seconds of turning). The black line is an exponential curve fitted to the data points.

Discussion:

Most of the analyzed terrains exhibit the characteristic shown in Figure 3. The current initially increases with the increase of rate, and then approaches a constant value. An exponential function of the form:

$$I = I_{\max}\left(1 - e^{-\frac{\omega}{K}}\right) \qquad (3)$$

can be fitted to the data points.

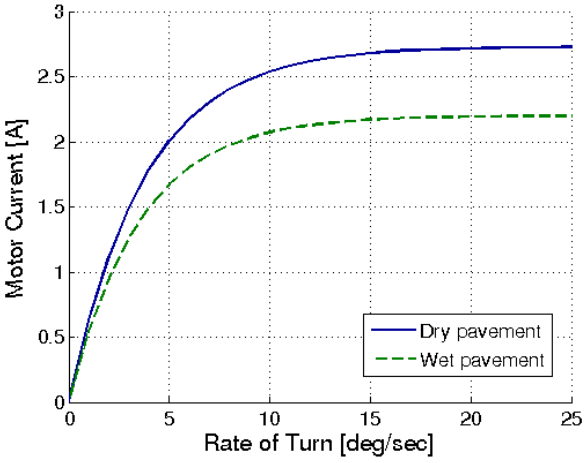

Figure 4: Rate of turn of the robot vs. average current on wet pavement and dry pavement.

Effects of changes in surface conditions

The MCR relationship can be affected considerably by many factors, such as moisture content, surface structure, or stratification (formation of layers) of soil. In order to demonstrate this point we collected data on pavement, before and after rainfall. The resulting MCR curves are clearly different, as shown in Figure 4. This can be a problem if the goal is terrain *classification*. However from the trafficability point of view, the two surface conditions are indeed different, even though they were measured on the same terrain.

Effects of changes in linear speed

Figure 5 shows that changes in the robot's linear speed also have a significant effect on the MCR curves. In the experiment of Figure 5 we ran the robot at three different speeds: 10 cm/sec, 20 cm/sec, and 40 cm/sec. The differences in the resulting MCR curves exist because at lower speeds the torque necessary for turning a skid-steer robot is higher than at higher speeds.

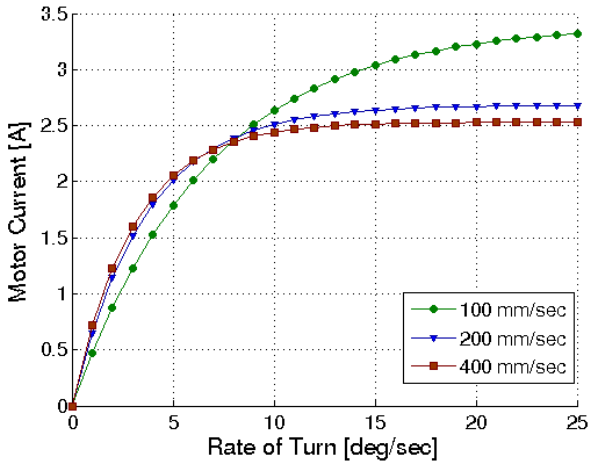

Figure 5: Motor Current vs. Rate of Turn curves at different linear speeds.

3. REAL TIME IMPLEMENTATIONS

A drawback of the above described proof-of-concept method is that it requires a significant amount of time and ample physical space. In this section we present two methods that overcome these limitations.

3.1 The Fast Spiral Path (FSP) Method

The FSP method is the real-time implementation of the basic proof-of-concept experiment discussed in Section 2. The only difference is that the robot stays at each rate of turn for shorter periods of time. We found that the MCR relationship is not affected significantly when using shorter periods for each commanded rate of turn (see Figure 6). Indeed, the rate of turn could change continuously, without affecting the results. However, the P2AT imposes some technical limitations on changes of the rate of turn: the maximum update rate of the internal microcontroller of the P2AT is 10 commands/sec, and the robot can only be commanded to increase rates of turn in increments of 1 deg/sec. In addition to reducing the time necessary for collecting the data, the FSP method also reduces the size of the terrain area necessary to collect the data, as shown in Figure 7.

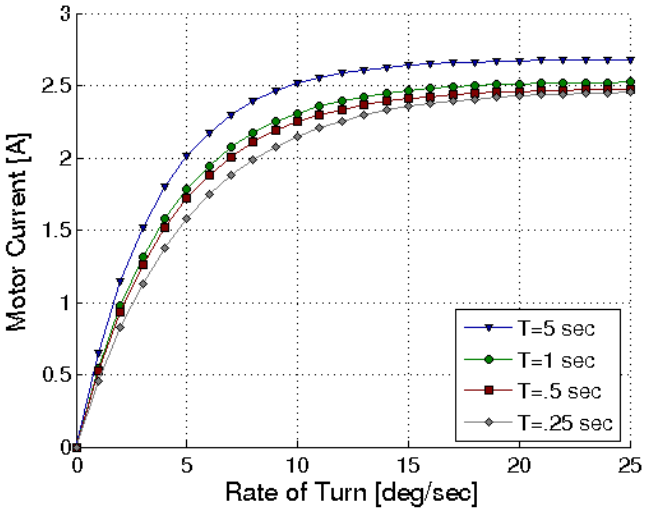

Figure 6: Motor current vs. rate of turn curves at different lengths of periods, at which each rate of turn is held constant.

A trade-off exists between the amount of measurement noise and the length of periods, at which each rate of turn is held constant, especially on noisy terrain such as grass or gravel. Longer constant-rate periods allow some averaging of the motor current and rate of turn data pairs, thereby significantly reducing the effect of noise. With very short constant-rate periods, on the other hand, the MCR curve is noisy since the FSP method relies on fewer samples per rate of turn. Such noisy data can result in similar terrains producing different results.

Even though noise is a potential problem for the FLP method, the statistic variance of the signal is characteristic for each type of terrain. This means that it can be used to help characterize the terrain, as will be demonstrated in Section 4.1 .

3.2 The Variable Frequency Rate of Turn (VFR) Method

For the *Variable Frequency Rate–of-turn* (VFR) approach the robot is subject to varying-frequency sinusoidal rates of turn commands. Specifically, the P2AT was commanded to move straight at constant speed with a sinusoidal rate of turn command overlaid over the straight motion command. The commanded and actual rates of turn, for an experiment on pavement, are shown in Figure 8. The frequency of the sinusoidal rate (see Figure 9) changed according to

$$T = T_0 - k\,\Delta t \qquad (4)$$

$$F = \frac{1}{T}, \quad T = 1,2,...n \qquad (5)$$

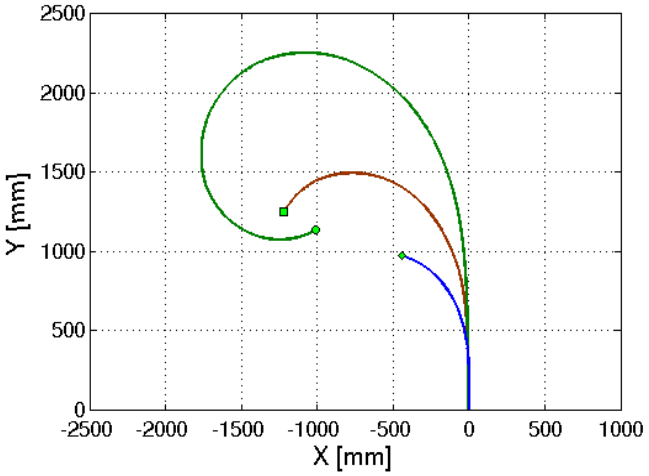

Figure 7: Path described by the robot during the Fast Spiral Path experiments, at different lengths of periods, at which each rate of turn is held constant.

where

T_0 – Initial period

Δt – Period step

k – Sampling interval index

As is evident from Figure 8, the P2AT is only able to follow the commanded rates of turn up to about 1.5 Hz. At higher frequencies the robot fails to react at all. Thus the experiments should be restricted to the range of very low frequencies, which is where most of the information is located, anyway.

When the robot is completely at rest, the motor currents have to increase significantly before the robot starts turning. This is because it has to develop enough torque to overcome friction, which is particularly large in a skid/steer robot starting from standstill. Once the robot moves, only small current increments are necessary to produce large rate variations. Furthermore, when the robot *reduces* its rate of turn, the interaction between the wheels and the terrain is quite different from the interaction while *increasing* the rate of turn. Thus, the plots of rate-versus-current look different in both cases. Since our procedure should be analogous to the one used in terramechanics with bevameters, we concluded that we should consider only the part of the sinusoidal cycle, during which the robot increases its angular rate.

As explained above, data collected with the VFR method must be segmented, so that only data associated with increasing rates of turn is considered. Thus, in each complete sinusoidal cycle there are two segments of data that we are interested in:

1. the increase of the rate of turn from zero deg/sec to the greatest positive rate, and
2. the "increase" of the rate of turn from zero deg/sec to the greatest negative rate.

In order to identify these segments within our raw data, we applied some heuristic rules that find the appropriate segments automatically. Figure 10 shows the result of applying this approach on pavement.

The VFR approach takes advantage of the best features of the slow proof-of concept experiment and the faster implementation of that approach, the FSP method. Specifically, the VFR method allows collecting redundant data through multiple sinusoidal cycles, while still being of short duration, since the rate of turn is varied rapidly and continually. Another advantage is that it doesn't impose large changes in the trajectory. Rather, it is realistically feasible to apply this method while the robot moves toward a goal. The sinusoidal path perturbations imposed by the VFR method cause only small deviations from the desired straight line path during a mission, as shown in Figure 11. Although this procedure can be performed at a fixed frequency, we found that by varying the frequency we can obtain additional

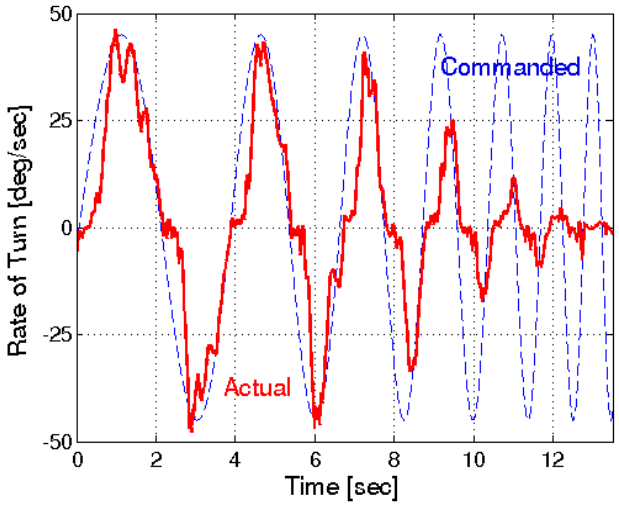

Figure 8: Commanded (blue) and actual (red) rate of turn.

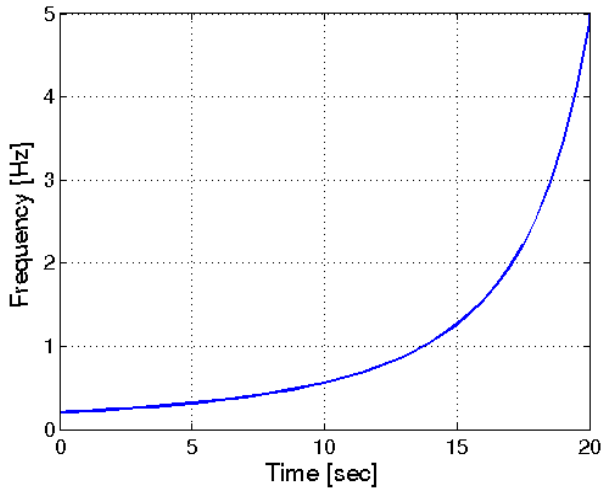

Figure 9: Sinusoidal rate frequency vs. time

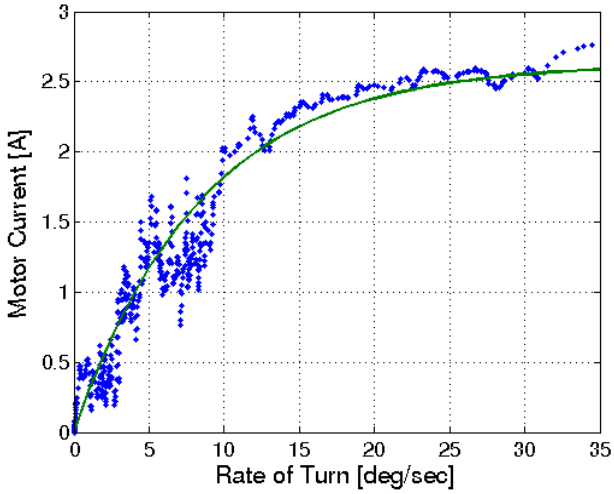

Figure 10: Plot of the MCR curve characteristic on pavement using the VFR method.

Table I: Comparison of methods for MCR data collection

	Spiral Path		Variable Frequency Rate of Turn (VFR)
	(Slow) proof-of-concept experiment	Fast Spiral Path method (FSP)	
Duration of experiment	Longest procedure (> 70 sec)	Fastest procedure (< 8 sec)	Short time (~10 sec)
Physical area required (forward × lateral direction)	Most area: (>6 x 6 m)	Less area (<1.5 x 1.5 m)	Least area (2 x 0.5 m)
Deviation from straight-line trajectory.	Large	Less	Least
Provides redundant information	Yes	No	Yes
Information for Variance analysis	Available	Very limited	Available
Slippage/skid analysis at different frequencies	No	No	Yes

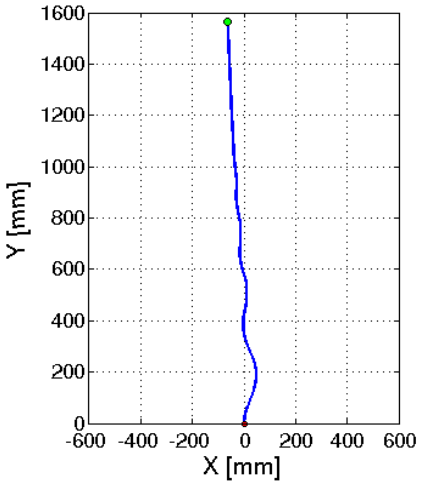

Figure 11: Path of the robot during a VFR experiment.

information about the terrain, as will be shown in Section 4.

Table I provides a qualitative comparison of the methods used for generating the MCR curves. The VFR is method is clearly the one that is best suited for real-time, in-mission applications. This is because it is fast, requires only a small area, and doesn't impose significant deviations from a nominal straight-line path.

4. EXPERIMENTAL RESULTS

In this section we present and analyze experimental data collected on five different terrains: gravel, grass, dirt, loose sand, and pavement. In all cases the VFR approached was used since any analysis applicable to the slow or fast versions of the Spiral Path method is applicable to the VFR method, whereas the opposite is not true. Figure 12 shows the Pioneer 2-AT skid-steer mobile robot that was used in all experiments described in this paper.

The resulting MCR curves for each terrain are shown in Figure 13. Data for this experiment was collected with the robot moving at a linear speed of 100 mm/sec, the amplitude of the sinusoidal rate commands was 45 deg/sec, and the frequency varied according to Eq. 5. For each surface type we collected several data sets, each from a different area of the same surface type, at least two meters away from any area used for any other data set.

In a deviation from the theoretical approach outlined in Section 2, we found that the exponential function approximation (Eq. 3) does not always fit very well the raw experimental data. For this reason we fitted a third order polynomial function of the form:

$$I_{pol} = k_1\omega^3 + k_1\omega^2 + k_1\omega^1 + k_1 \qquad (6)$$

Although the polynomial curves provide a better-looking representation of the data, there are two disadvantages to representing the data by the polynomials *exclusively*:

1. the noise level of the signal is not present (yet, noise contains useful information, as shown below), and
2. when the data is very noise, polynomials may not make for a good fit for the raw data.

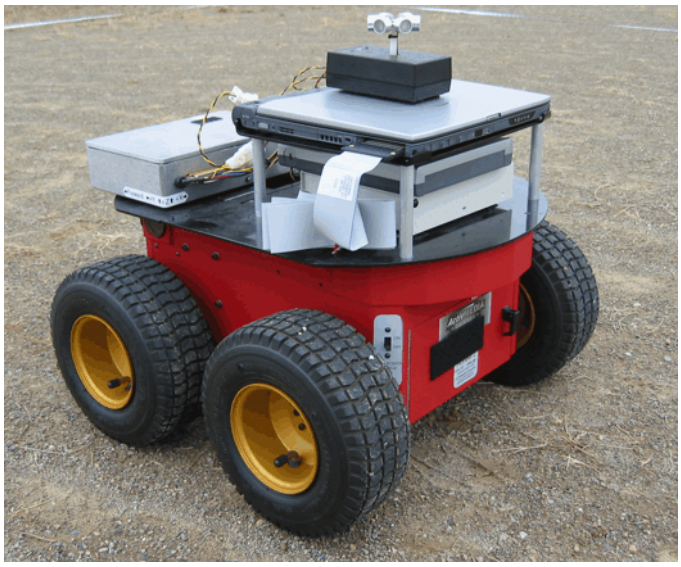

Figure 12: The Pioneer 2-AT skid-steer mobile robot used in all of our experiments.

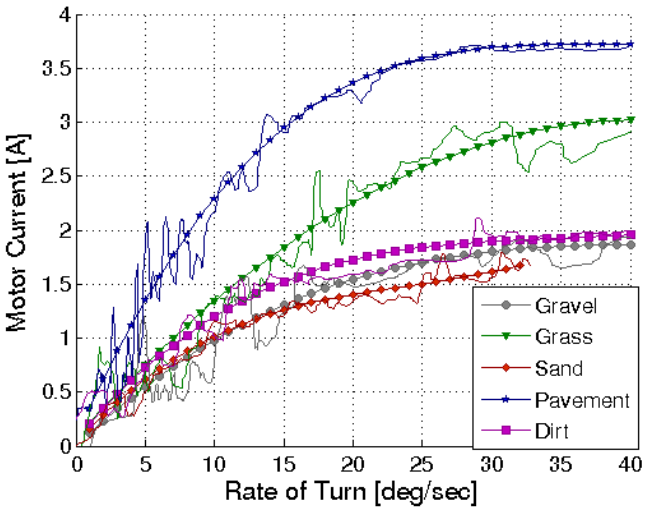

Figure 13: MCR curve characteristic for different terrains (dotted lines), collected with the VFR method. Solid curves are polynomials fitted to the data for each terrain.

Nonetheless, we think that the polynomials are useful as long as we present them together with the data that was used to generate them, as is the case in Figure 13.

4.1 Distinguishing Gravel

Among the MCR curves of Figure 13, the curves for pavement and grass can be distinguished easily. However, the curves for soil, gravel, and sand are very similar and overlap. Therefore, additional information is needed to classify these surfaces.

We found that a good method for determining whether a certain MCR curve represents gravel is by looking at the variance of its data. This is so because the amount of noise on gravel is considerably larger than that of noise on sand and dirt. Figure 14 shows the MCR curves for several experiments collected on dirt, gravel, and sand. We found that in all experiments the standard deviation of the signal on gravel was up to twice as large as that of sand or soil.

Figure 15 shows the variance of the MCR curve for the three different terrains. We computed the variance as the standard deviation of the difference between the raw data and a third order polynomial fit (Eq. 6):

$$\delta = std\left(I_{pol} - I\right) \qquad (7)$$

On average, dirt produces the lowest noise level. However, in some cases sand also produces low noise levels. Therefore noise is not a sufficient criterion for distinguishing between dirt and sand.

To overcome this problem, we looked for an additional criterion to distinguish between dirt and sand, and we found one in the form of wheel encoder information. In the following section we discuss how this approach works.

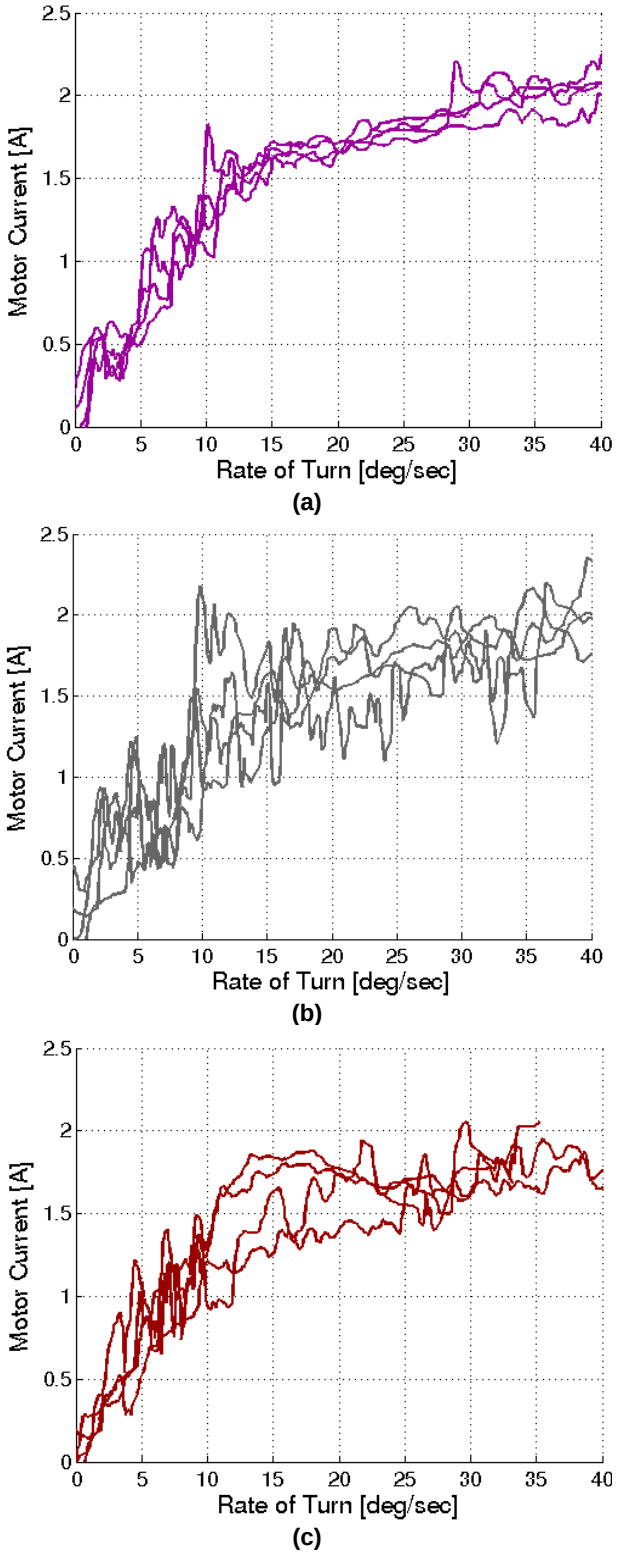

Figure 14: MCR curves for: a) dirt, b) gravel, and c) sand. In each graph we show four independent runs on the specified terrain.

4.2 Distinguishing between sand and dirt

In order to distinguish between sand and dirt, we define:

$$\omega_{diff} = \omega_g - \omega_{odo} \quad (8)$$

where

ω_{odo} - rate of turn computed from encoder data

ω_g - rate of turn measured by the Z-axis gyroscope,

ω_{diff} - discrepancy between the above two rates of turn

A value of $\omega_{diff} = 0$ represents no slippage or skid. In practice, there is always a difference due to the noise in the signals and due to the discrete resolution of the sensors. $\omega_{diff} > 0$ means that the encoders did not register part of the rotation of the robot. This situation is more likely to be found at high rates of turn where some skid may occur or the wheels may deform due to the high torques applied by the ground. A value of $\omega_{diff} < 0$ is generally associated with slippage, which is more likely to occur when the robot is subject to sudden rotations, as in the case of high frequency rates of turn.

Figure 16 shows a plot of the rate difference for all surfaces as a function of the rate of turn frequency. The rate difference was obtained at the points where the rate of turn reached the maximum value (positive or negative). We can see that for most surfaces some skid occurs at the low frequencies ($\omega_{diff} > 0$) and that the robot is more likely to slip at higher rates ($\omega_{diff} < 0$). However, on loose sand the robot slips at low and high frequencies – a unique feature that can be used to determine when the robot is driving on sand.

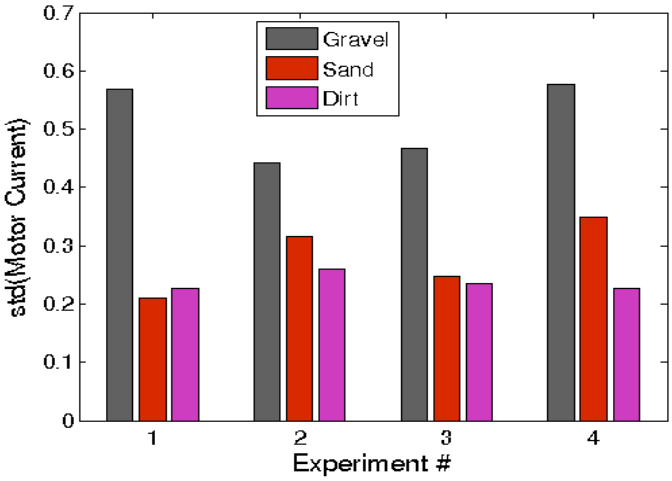

Figure 15: Signal noise level for different surfaces.

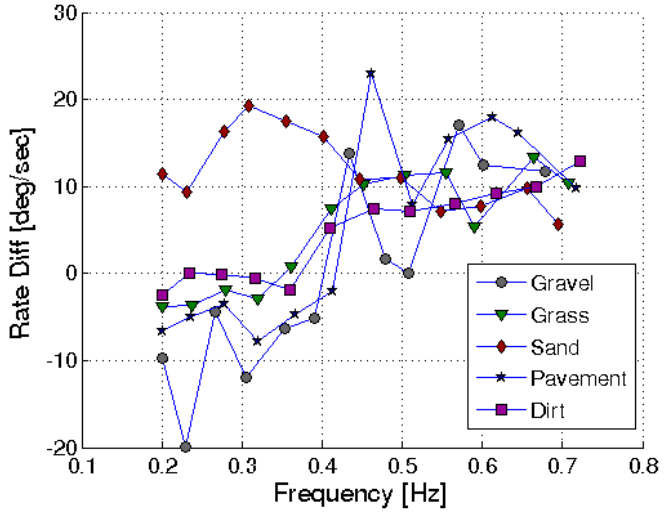

Figure 16: Rate of turn difference on different surfaces vs. rate of turn frequency.

5. CONCLUSIONS

This paper examined different methods for characterizing terrains with regard to trafficability for small mobile robots. On skid-steer mobile robots, the proposed methods can be used in real-time, during an actual mission.

Terrains are characterized by what we call Motor Current vs. Rate of turn (MCR) curves, which are similar to the strain-stress curves used in terramechanics. Among the two proposed methods for generating MCR curves we found that the Variable Frequency Rate of turn (VFR) method was significantly more suitable for real-time application than the alternative Fast Spiral Path (FSP) method. We believe that the VFR data collection method contains sufficient information for classifying the five test surfaces, although we did not address classification in this paper.

Acknowledgements:

This research was performed under subcontract to Turing Associates, Inc., of Ann Arbor, MI, as part of SBIR contract DAAE07-02-C-L003 to the U.S. Army RDECOM (TARDEC). Publication of these results does not constitute endorsement by an agency or official of the U.S. Government.

6. BIBLIOGRAPHY

Bekker, G., 1956, "Theory of Land Locomotion." *University of Michigan Press*, Ann Arbor, MI.

Bekker, G., 1960, "Off the Road Locomotion." *University of Michigan Press*, Ann Arbor, MI.

Bekker, G., 1969, "Introduction to Terrain-Vehicle Systems." *University of Michigan Press*, Ann Arbor, MI.

Iagnemma, K., Kang, S., Shibly, H., and Dubowsky, S., 2004, "On-line Terrain Parameter Estimation for Planetary Rovers." *IEEE Transactions on Robotics*, October, vol. 20, no. 2, pp. 921-927.

Janosi, Z., and Hanamoto, B., 1961, "Analytical Determination of Drawbar Pull as a Function of Slip for Tracked Vehicles in Deformable Soils." *Proc. First Int. Conf. On Terrain-Vehicle Systems*, Torino, Italy.

Manduchi, R., Castano, A., Talukder, A., Matthies, L., 2005, "Obstacle Detection and Terrain Classification for Autonomous Off-Road Navigation." *Autonomous Robots*.

Moore, H., Hutton, R., Scott, R., Spitzer, C., and Shorthill, R., 1977, "Surface Materials of the Viking Landing Sites." *Journal of Geophysical Research*, Vol. 82, No. 28, pp. 4497-4523

Nohse, Y., Hashuguchi, K., Ueno, M., Shikanai, T., Izumi, H., and Koyama, F. 1991, "A measurement of basic mechanical quantities of off-the-road traveling performance." *Journal of Terramechanics,* vol. 28, no. 4, pp. 359–370.

Shmulevich, I.; Ronai, D.; and Wolf, D; 1996, "A new field single wheel tester." *Journal of Terramechanics*, vol. 33, no. 3, pp. 133–141.

Vandapel, N., Huber, D., Kapuria, A. and Hebert, M., 2004, "Natural Terrain Classification using 3-D Ladar Data." Proc. *IEEE Int. Conf. on Robotics and Automation,* pp. 5117-5122

Wong, J., Reece A., 1967, "Prediction of Rigid Wheel Performance Based on the Analysis of Soil-Wheel Stresses, Part I and Part II." *Journal of Terramechanics*, vol. 4(1): pp. 81-98, vol. 4(2): pp. 7-25.